AIP | Applied Physics Letters

Phase-change memory devices based on gallium-doped indium oxide

S.-L. Wang, C.-Y. Chen, M.-K. Hsieh, W.-C. Lee, A. H. Kung, and L.-H. Peng

Citation: Applied Physics Letters **94**, 113503 (2009); doi: 10.1063/1.3089238
View online: http://dx.doi.org/10.1063/1.3089238
View Table of Contents: http://scitation.aip.org/content/aip/journal/apl/94/11?ver=pdfcov
Published by the AIP Publishing

Phase-change memory devices based on gallium-doped indium oxide

S.-L. Wang,[1,2] C.-Y. Chen,[1] M.-K. Hsieh,[3] W.-C. Lee,[3] A. H. Kung,[2,4] and L.-H. Peng[1,a)]
[1]*Department of Electrical Engineering, Institute of Photonics and Optoelectronics, National Taiwan University, Taipei 106, Taiwan, Republic of China*
[2]*Institute of Atomic and Molecular Sciences, Academia Sinica, Taipei 106, Taiwan, Republic of China*
[3]*Exploratory Research Division, Taiwan Semiconductor Manufacturing Company, Ltd., Hsinchu 300, Taiwan, Republic of China*
[4]*Department of Photonics, National Chiao Tung University, Hsinchu 300, Taiwan, Republic of China*

(Received 11 September 2008; accepted 5 February 2009; published online 18 March 2009)

We report repetitive phase-change memory (PCM) activity via the high- to low-resistance state transition in gallium-doped indium oxide (Ga:InO) induced by nanosecond electric pulses. The amorphous-to-crystalline phase transition of Ga:InO is found to occur at a crystallization temperature of ~250 °C with an activation energy of 1.27 ± 0.07 eV. At the phase transition, we observe a change in two orders of magnitude in the PCM-device resistance, which can be correlated with the formation of (211) and {222} crystallites of bixbyite cubic In_2O_3. We ascribe the phase-change mechanism to the Joule heating effect in Ga:InO. © *2009 American Institute of Physics*. [DOI: 10.1063/1.3089238]

Tellurium-based phase-change memory (PCM) materials composed of germanium antimony tellurium (GST) compounds have long been considered for applications in optical data storage. Phase-change random access memory is known to offer a switching speed that is 100 times faster than that of flash memory and it is likely to replace flash memory beyond the 45 nm technology nodes.[1–5] The underlying physics involves the reflectivity or resistance of a PCM device, which can be set/reset between two high/low levels due to a reversible change between the crystalline and the amorphous states by external stimuli. Earlier investigations suggested that through nitrogen doping, one can reduce the switching current due to an increase in GST film resistivity.[6] The activation energy for amorphous to face-centered cubic crystallization for a GST film can also be increased by mixing with silicon suboxide (SiO_x), thus leading to a reduction in the programming current and an increase in film stability.[7] More recently, there has been increasing interest in using suboxide films as the optical recording medium for blue-ray disk applications. Write-once disks based on tungsten oxide (WO_2) and antimony oxide (SbO_x) have been demonstrated.[8–10] It is of interest to explore whether oxide-based PCM devices could be made to offer repetitive set/reset activity due to the reversible structure change.

Crystalline indium oxide (In_2O_3) is known to have a cubic structural symmetry and it acts as an *n*-type material due to the oxygen-vacancy effect.[11] Although optical recording based on the metal-insulator transition[12] or metallic percolation[13] was reported earlier for tin-doped indium oxide and metal/InO_x composites, the memory activity that causes reversible structural change has not been identified in this system. In this work, we report nonvolatile PCM activity based on a reversible change between the amorphous and the cubic (bixbyite) phases of gallium-doped indium oxide (Ga:InO). Device switching between the low- and high-resistance states for over 300 cycles has been verified in a Ga-doped In_2O_3 PCM cell with a Ga/(In+Ga) ratio=0.2%. With high resolution transmission electron microscopy (HRTEM) analysis, we determined that the lattice images confirm that reversible changes can be made between the crystalline and amorphous phases of the Ga:InO material. We ascribe the phase-change mechanism to Joule heating by pulsed electrical current in Ga:InO.

The Ga:InO PCM devices used in this work were prepared by cosputtering indium oxide and gallium oxide into a cell structure that was bottom-contacted with a rodlike tungsten (W) heater with a diameter of 1.6 μm on a (111) silicon substrate. The Ga composition in Ga:InO films can be varied by controlling the rf power and the oxygen flow rate. For example, at an oxygen flow rate of 5 SCCM (SCCM denotes standard cubic centimeter per minute at STP) and rf power of 35 W, the as-grown Ga:InO film appeared to be amorphous and had an atomic ratio of Ga:(In+Ga)=1:10, as determined by energy-dispersive x-ray analysis. We applied a circular transmission line method and x-ray diffraction (XRD) to examine the change in film resistivity and crystallinity with annealing temperature. This procedure facilitates the determination of the crystallization temperature of the Ga:InO film. This information, along with data taken by differential scanning calorimetry (DSC), allowed us to determine the phase-change activation energy in Ga:InO.

Electrical characterization of Ga:InO devices was performed by using an Agilent 4155C semiconductor analyzer for dc and an Agilent 81110A programmable pulse generator for pulsed *I-V* analysis, respectively. For the latter, a load resistance R_L of 1 kΩ was put in series with the PCM device and the current that flowed through the device was determined from the voltage drop across R_L, which was measured using a digital oscilloscope.[4] The cell resistance R of the PCM device was then measured at a low current level ~1 μA. This procedure allowed us to characterize the resistance change after the device was subjected to an electrical pulse.

Figures 1(a) and 1(b) show the dc characteristics for two Ga:InO devices with Ga-doping compositions of ~0.2% and 5%, respectively. These devices were constructed to have a cell area of 2 μm^2 and a 20 nm film thickness. Beginning at

a)Electronic mail: peng@cc.ee.ntu.edu.tw.

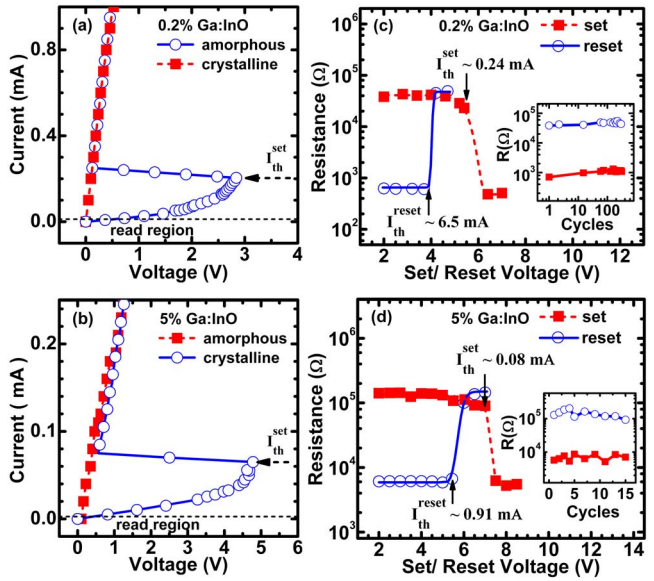

FIG. 1. (Color online) [(a) and (b)] *I-V* and [(c) and (d)] pulsed *R-V* plots for 0.2% and 5% Ga:InO devices. The device dimension is ~2 μm^2 in area and 20 nm in film thickness. Inset: cycling data from the 0.2% and 5% Ga:InO PCM device.

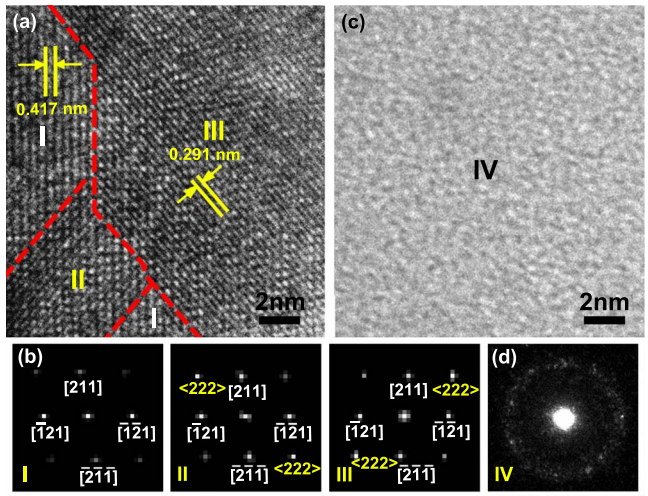

FIG. 2. (Color online) [(a) and (c)] Cross-sectional HRTEM lattice images of 0.2% Ga:InO devices A and B prepared in the low and high-resistance states, respectively, (b) reciprocal space structure mapping by Fourier transform of the lattice image of device A and (d) the SAED data for device B.

the as-grown high-resistance (reset) state, the *I-V* plots display an S-shaped negative differential resistance followed by a sudden drop in voltage once the threshold-switching point is reached. We observe from the *I-V* plots a drastic change in the threshold current and voltage (I_{th}, V_{th}) from (0.2 mA, 2.84 V) for the 0.2% Ga-doping concentration to (0.065 mA, 4.78 V) for the 5% Ga-doping concentration. Beyond this threshold point, we encountered a low-resistance (set) state of Ga:InO, which exhibits a linear slope on the *I-V* plot.

Indeed, the aforementioned dc-conductivity behavior of the Ga:InO device resembles that of GST devices where a similar characteristic change in the *I-V* plot has been associated with a change from the amorphous to the crystalline phase.[4] A change in resistance of two orders of magnitude due to switching between the reset/set states of the Ga:InO devices justifies the potential use of this material system for PCM applications. Indeed, the resistance window of Ga:InO devices, which was extracted from the pulsed *R-V* data, was found to change with Ga concentration. The resistance window of the (reset, set) state shifts from $(\sim 4 \times 10^4\ \Omega, \sim 6 \times 10^2\ \Omega)$ in Fig. 1(c) for a 0.2% Ga:InO device to $(\sim 1.3 \times 10^5\ \Omega, \sim 6 \times 10^3\ \Omega)$ in Fig. 1(d) for a 5% Ga:InO device. A corresponding change in the threshold value of the set/reset electric pulse was also found: (5.4 V, 0.24 mA) at 80 ns in width and (3.9 V, 6.5 mA) at 20 ns in width for the 0.2% Ga:InO device to (7 V, 0.08 mA) at 80 ns and (5.4 V, 0.91 mA) at 20 ns for the 5% Ga:InO device. The reported voltage is the voltage drop across the cell. Note that the discrepancy between the dc and the pulse set/reset *I-V* data shown in Fig. 1 may reflect the device parasitic capacitance effect in the programming electric pulses.[14]

It is noted that data of the resistance window for the Ga:InO PCM devices shown in Figs. 1(c) and 1(d)were measured at a fixed device size with a bottom electrode area of 2 μm^2 and film thickness of 20 nm. In a separate experiment, we measured the resistivity of 3 and 60 Ω cm, respectively, for the 0.2% and 5% Ga:InO film which was prepared into the crystalline state, whereas over two orders of magnitude increase in the film resistivity can be observed when the film was prepared into the amorphous state. This analysis indicates that the resistivity of the Ga:InO film not only changes with the amorphous/crystalline state but also depends on the Ga composition of the Ga:InO film. The observation of resistance window change and shift in the Ga:InO PCM devices reflects the difficulty in pursuing phase changes in the Ga_2O_3 material.[15] The detailed mechanism of the resistivity shift in the high Ga-doped InO film is under investigation and will be presented in a forthcoming publication

It nevertheless points to the promising PCM application of this material system, as shown in the inset of Fig. 1(c), where electric cycling over 300 times has been conducted between the set/reset states of a 0.2% Ga:InO device. The electric cycling data for the 5% Ga:InO PCM device were included in the inset of Fig. 1(d) and showed that a cycling endurance of 15 times can be achieved. However, this number is less than that of 300 times cycling endurance measured on the 0.2% Ga:InO device and may be due to a nonoptimized electric pulse condition. The detail of failure mechanism is still under investigation.

Indeed, the *I-V* characteristics shown in Fig. 1 for the Ga:InO device resemble those earlier reported for the GST-based PCM device.[1–5] To understand the effect of crystallinity on the phase transition behavior, we applied cross-sectional HRTEM analysis to another set of two 0.2% Ga:InO devices, devices A and B that were prepared separately in the low and high-resistance states by repetitive electric pulses. Large-angle grain boundaries that split the lattice fringes with spacings of d=4.17 and 2.91 Å, corresponding to the (211) and (222) crystalline plane of bixbyite cubic phase In_2O_3, respectively, were observed by HRTEM [Fig. 2(a)] in the low-resistance device A.[16] A close examination of zones II and III in Fig. 2(a) reveals Moiré fringe patterns which signify interference due to the overlap of two or more grains of different orientations.[17] Subtleties such as this can be resolved by taking a Fourier transform of the lattice image to project the reciprocal space structures.[18] By doing so, we mapped out in Fig. 2(b) the reciprocal space geometries and identified the constituents as (i) single grains of (211) In_2O_3

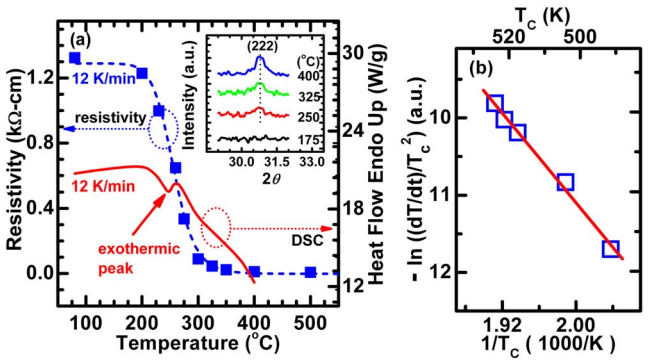

FIG. 3. (Color online) (a) Temperature-dependent resistivity of the 0.2% Ga:InO film overlaid with data measured by DSC analysis. Inset: XRD spectra near the crystallization temperature. (b) Kissinger's plot of the 0.2% Ga:InO film to facilitate the extraction of the activation energy.

crystallites in zone I and (ii) mixed grains in zones II and III, each containing an overlap of (211) and {222} In_2O_3 crystallites.[19] This result shows the formation of crystallite grains in an amorphous matrix background; instead of a crystalline rim surrounding the amorphous region and this suggests a nucleation-dominated mechanism[2] for the crystallization of the Ga:InO material system. In comparison, for device B prepared in a high-resistance state, the selected area electron diffraction (SAED) data in Fig. 2(d) exhibits a scattered ringlike pattern, characteristic of an amorphous state that results from a rapid quenching of the melt.[20]

These observations suggest that the origin of electrically driven memory activity in Ga:InO cells, as in the case of the GST-based PCM cells reported earlier is related to the Joule heating effect.[21] To verify this proposed mechanism, we examined the effect of thermal heating on the resistivity and XRD spectra of a Ga:InO film and compared the results with the exothermic reaction data obtained by DSC analysis. Samples were subjected to vacuum annealing at a heating rate of 12 K/min. We found a threshold behavior in the 0.2% Ga:InO film where the resistivity changed from 1.3×10^3 to 3 Ω cm, as shown in Fig. 3(a). From the inflection point in the resistivity curve,[7] we determined a crystallization temperature of $T_c\sim252$ °C. Around this transition temperature, we observed the onset of an XRD signal at $2\theta=30.7°$, corresponding to diffraction from the (222) plane of the cubic phase In_2O_3,[22] as shown in the inset of Fig. 3(a). Unlike the GST film, which undergoes a structural change first from an amorphous phase to a rock salt structure at 140 °C; then to a hexagonal structure at 310 °C,[23] the amorphous Ga:InO film underwent only one crystalline transition to cubic In_2O_3. Facilitated by the DSC analysis taken at a heating rate dT/dt of 12 K/min, we identified an exothermic peak at 248 °C, close to the crystallization temperature ($T_c\sim252$ °C) of the Ga:InO film. These observations, together with the HRTEM analysis, suggest that the Joule heating effect is responsible for the amorphous-to-crystalline structural change in the Ga:InO PCM system. Indeed, from the Kissinger's plot[24] [as shown in Fig. 3(b)], by semilogarithmic fitting of the heating rate $\ln[(dT/dt)/T_C^2]$ versus $1/T_C$ curve, we can derive an activation energy of $E_a=1.27\pm0.07$ eV for the Ga:InO PCM film. Detailed analyses of the retention time of the Ga:InO PCM device will be presented in a forthcoming publication.

In summary, we report the repetitive switching behavior between the high-resistance (amorphous) and low-resistance (crystalline) states in PCM devices made of Ga:InO. Electrical pulses at 5.4 V with a duration of 80 ns and 3.9 V with a duration of 20 ns were shown to enable the phase transition process in 0.2% Ga:InO cells with an area of 2 μm^2 and a thickness of 20 nm. The amorphous to bixbyite cubic In_2O_3 phase transition was found to take place at a crystallization temperature of 252 °C and an activation energy of 1.27 ± 0.07 eV. We ascribe the phase-change mechanism to the Joule heating effect in Ga:InO.

This research was supported by the National Science Council Contract No. 97–2221-E-002–045 and TSMC-NTU Grant No. 94-FS-B05, B15 and Aim for Top University Project from the Ministry of Education, Republic of China

[1] A. Redaelli, A. Pirovano, A. Benvenuti, and A. L. Lacaita, J. Appl. Phys. **103**, 111101 (2008).
[2] W. Welnic and M. Wuttig, Mater. Today **11**, 20 (2008).
[3] A. V. Kolobov, Nature Mater. **7**, 351 (2008).
[4] M. H. R. Lankhorst, B. W. S. M. M. Ketelaars, and R. A. M. Wolters, Nature Mater. **4**, 347 (2005).
[5] S. Lai, Tech. Dig. - Int. Electron Devices Meet. **2003**, 10.1.1.
[6] H. Horii, J. H. Park, J. H. Yi, B. J. Kuh, and Y. H. Ha, IEICE Trans. Electron. **E87-C**, 1673 (2004).
[7] T. Y. Lee, S. S. Yim, D. Lee, M. H. Lee, D. H. Ahn, and K. B. Kim, Appl. Phys. Lett. **89**, 163503 (2006).
[8] T. Ohta, M. Takenaga, N. Akahira, and T. Yamashita, J. Appl. Phys. **53**, 8497 (1982).
[9] T. Aoki, M. Tatsuhiko, A. Suzuki, T. Kenji, and M. Okuda, Thin Solid Films **509**, 107 (2006).
[10] Y. Zhou, Y. Y. Geng, D. H. Gu, Q. Zhu, and Z. Jiang, Appl. Surf. Sci. **254**, 1369 (2007).
[11] A. N. H. Al-Ajili and S. C. Bayliss, Thin Solid Films **305**, 116 (1997).
[12] M. C. de Andrade and S. Moehlecke, Appl. Phys. A: Solids Surf. **58**, 503 (1994).
[13] A. F. Hebard, G. E. Blonder, and S. Y. Suh, Appl. Phys. Lett. **44**, 1023 (1984).
[14] D. Ielmini, D. Mantegazza, A. L. Lacaita, A. Pirovano, and F. Pellizzer, IEEE Electron Device Lett. **26**, 799 (2005).
[15] L. Nagarajan, R. A. De Souza, D. Samuelis, I. Valov, A. Borger, J. Janek, K. D. Becker, P. C. Schmidt, and M. Martin, Nature Mater. **7**, 391 (2008).
[16] S.-L. Wang, C.-Y. Chen, M.-K. Hsieh, W.-C. Lee, A.-H. Kung, and L.-H. Peng, Technical Digest 23rd IEEE Non-Volatile Semiconductor Memory Workshop, 2008 (unpublished), p. 33.
[17] S. Raoux, C. T. Rettner, J. L. Jordan-Sweet, A. J. Kellock, T. Topuria, P. M. Rice, and D. C. Miller, J. Appl. Phys. **102**, 094305 (2007).
[18] Digital Micrograph V. 3.6.4, GATAN software, 1999.
[19] CaRIne Crystallography V. 3.1, CARINE software, 1998.
[20] P. Haasen, *Physical Metallurgy* (Cambridge University Press, Cambridge, 1986), p. 79.
[21] S. B. Kim and H.-S. P. Wong, IEEE Electron Device Lett. **28**, 697 (2007).
[22] JCPDS Card No. 44–1087.
[23] I. Friedrich, V. Weidenhof, W. Njoroge, P. Franz, and M. Wuttig, J. Appl. Phys. **87**, 4130 (2000).
[24] H. E. Kissinger, Anal. Chem. **29**, 1702 (1957).